The Patent Office
Concept House
Cardiff Road
Newport
South Wales
NP10 8QQ

I, the undersigned, being an officer duly authorised in accordance with Section 74(1) and (4) of the Deregulation & Contracting Out Act 1994, to sign and issue certificates on behalf of the Comptroller-General, hereby certify that annexed hereto is a true copy of the documents as originally filed in connection with the patent application identified therein.

In accordance with the Patents (Companies Re-registration) Rules 1982, if a company named in this certificate and any accompanying documents has re-registered under the Companies Act 1980 with the same name as that with which it was registered immediately before re-registration save for the substitution as, or inclusion as, the last part of the name of the words "public limited company" or their equivalents in Welsh, references to the name of the company in this certificate and any accompanying documents shall be treated as references to the name with which it is so re-registered.

In accordance with the rules, the words "public limited company" may be replaced by p.l.c., plc, P.L.C. or PLC.

Re-registration under the Companies Act does not constitute a new legal entity but merely subjects the company to certain additional company law rules.

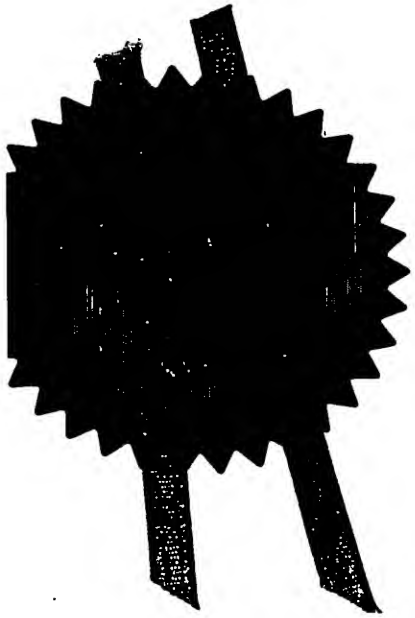

Signed

Dated 9 July 2004

Patents Form 1/77

Patents Act 1977
(Rule 16)

THE PATENT OFFICE
CR
25 JUL 2003
RECEIVED BY FAX

The Patent Office

1/77

Request for grant of a patent

(See the notes on the back of this form. You can also get an explanatory leaflet from the Patent Office to help you fill in this form)

25 JUL 2003

The Patent Office
Cardiff Road
Newport
South Wales
NP9 1RH

1. Your reference
LRD-GB-1-455

2. Patent application number *(The Patent Office will fill in this part)* 0317467.9

25JUL03 E925463-1 D10059
P01/7700 0.00-0317467.9

3. Full name, address and postcode of the or of each applicant *(underline all surnames)*
K.U.Leuven Research and Development - Groot Begijnhof 59 - 3000 Leuven
Represented by Dr. Ivo Roelants, IPR Officer
Patents ADP number *(if you know it)*

If the applicant is a corporate body, give the country/state of its incorporation Belgium 07665649003

4. Title of the invention
Tissue infarction and necrosis specific compounds

5. Name of your agent *(if you have one)*
K.U.Leuven R&D
care off:
Hubert Velge
Neaves Cottage
Neaves Lane - Glyndebourne
East Sussex BN8 5UA

"Address for service" in the United Kingdom to which all correspondence should be sent *(including the postcode)*

Patents ADP number *(if you know it)* 08007916003

6. If you are declaring priority from one or more earlier patent applications, give the country and the date of filing of the or of each of these earlier applications and *(if you know it)* the or each application number

Country	Priority application number *(if you know it)*	Date of filing *(day / month / year)*

7. If this application is divided or otherwise derived from an earlier UK application, give the number and the filing date of the earlier application

Number of earlier application	Date of filing *(day / month / year)*

8. Is a statement of inventorship and of right to grant of a patent required in support of this request? *(Answer 'Yes' if:*
a) any applicant named in part 3 is not an inventor, or
b) there is an inventor who is not named as an applicant, or
c) any named applicant is a corporate body.
See note (d))

Yes

Patents Form 1/77

Patents Form 1/77

9. Enter the number of sheets for any of the following items you are filing with this form. Do not count copies of the same document

Continuation sheets of this form	
Description	1722
Claim(s)	—
Abstract	1
Drawing(s)	6

10. If you are also filing any of the following, state how many against each item.

Priority documents	
Translations of priority documents	
Statement of inventorship and right to grant of a patent *(Patents Form 7/77)*	2
Request for preliminary examination and search *(Patents Form 9/77)*	
Request for substantive examination *(Patents Form 10/77)*	
Any other documents *(please specify)*	1 fax cover sheet 1 fee sheet with request for fax back service

11. I/We request the grant of a patent on the basis of this application.

Dr. Ivo Roelants - IPR Officer

Signature Date 25.07.03

12. Name and daytime telephone number of person to contact in the United Kingdom

Hubert Velge
+44 7940 540 397

Warning

After an application for a patent has been filed, the Comptroller of the Patent Office will consider whether publication or communication of the invention should be prohibited or restricted under Section 22 of the Patents Act 1977. You will be informed if it is necessary to prohibit or restrict your invention in this way. Furthermore, if you live in the United Kingdom, Section 23 of the Patents Act 1977 stops you from applying for a patent abroad without first getting written permission from the Patent Office unless an application has been filed at least 6 weeks beforehand in the United Kingdom for a patent for the same invention and either no direction prohibiting publication or communication has been given, or any such direction has been revoked.

Notes

a) *If you need help to fill in this form or you have any questions, please contact the Patent Office on 0645 500505.*

b) *Write your answers in capital letters using black ink or you may type them.*

c) *If there is not enough space for all the relevant details on any part of this form, please continue on a separate sheet of paper and write "see continuation sheet" in the relevant part(s). Any continuation sheet should be attached to this form.*

d) *If you have answered 'Yes' Patents Form 7/77 will need to be filed.*

e) *Once you have filled in the form you must remember to sign and date it.*

f) *For details of the fee and ways to pay please contact the Patent Office.*

Tissue Infarction and Necrosis Specific Compounds

Field of the invention

The present invention concerns to the use of hypericin or its derivatives, preferably polycyclic aromatic anthrone analogues, as a necrosis specific or infarct specific agent and the use of hypericin or its derivatives in tissue infarction or tissue necrosis diagnosis or therapy. Hypericine or its derivatives can be labeled by a tracer, a radioactive compound, contrast agent or conjugated with a medical compound.

Background of the invention

St. John's Wort or *Hypericum Perforatum*, a widely growing erect perennial herb with golden yellow flowers, has been used for millennia to treat a variety of ailments including depression, bacterial and viral infections, as well as malignant tumors [G. Lavie, Y. Mazur, D. Lavie and D. Meruelo , The chemical and biological properties of hypericin: a compound with a broad spectrum of biological activities. Med. Res. Rev. 15 (1995), pp. 111–119.]. Among those claimed effective constituents of this herb, extracted and/or synthetic hypericin and pseudohypericin are polycyclic aromatic anthrone analogues, a class of pigmented chemical substances with photosensitizing property. When exposed to light, hypericin transfers energy to nearby oxygen molecules, creating very reactive "singlet" oxygen molecules that are toxic to biological structures. Based on this photosensitizing property early in last decade, hypericin was shown to be effective in killing certain tumors and many viruses [G. Lavie, Y. Mazur, D. Lavie and D. Meruelo , The chemical and biological properties of hypericin: a compound with a broad spectrum of biological activities. Med. Res. Rev. 15 (1995), pp. 111–119].

We now carried out an imaging-histomorphological correlation study to visualize hypericin tissue distribution. Such experiments on mammalian models by meticulous and accurate methodologies applied clearly demonstrated for the first time and proved that MIH proves to be a highly

sensitive/ specific necrosis-avid. By present invention Hypericin was demonstrated to be a Necrosis-avid contrast agent (NACA).

And although potential clinical impact of a necrosis-targeting approach has been repeatedly emphasized in the literature with other NACA's are known in the art [Ni Y, Marchal G, Yu J, Lukito G, Petré C, Wevers M, Baert AL, Ebert W, Hilger CS, Maier FK, Semmler W: Localization of metalloporphyrin induced "specific" enhancement in experimental liver tumors: a comparison between MRI, microangiographic and histologic findings. Acad Radiol 1995; 2: 687-699; NI Y, Petré C, Miao Y, Yu J, Cresens E, Adriaens P, Bosmans H, Semmler W, Marchal G: Magnetic resonance imaging-histomorphologic correlation studies on paramagnetic metalloporphyrins in rat models of necrosis. Invest Radiol 1997; 32(12): 770-779; Maurer J, Strauss A, Ebert W, Bauer H, Felix R. Contrast-enhanced high resolution magnetic resonance imaging of pigmented malignant melanoma using Mn-TPPS4 and Gd-DTPA: experimental results. Melanoma Res 2000; 10: 40-6; Marchal G, Ni Y. Use of porphyrin-complex or expanded porphyrin-complex as an infarction localization diagnosticum. U.S. patent No. 6,013,241; Marchal G, Ni Y, Herijgers P, Flameng W, Petré C, Bosmans H, Yu J, Ebert W, Hilger C-S, Pfefferer D, Semmler W, Baert AL: Paramagnetic metalloporphyrins: infarct avid contrast agents for diagnosis of acute myocardial infarction by magnetic resonance imaging. Eur Radiol 1996; 6: 2-8; Ni Y, Marchal G, Herijgers P, Flameng W, Petré C, Hilger CS, Ebert W, Maier FK, Semmler W, Baert AL: Paramagnetic metalloporphyrins: from enhancers for malignant tumors to markers of myocardial infarcts. Acad Radiol 1996; 3(8): S395-397; Herijgers P, Laycock SK, Ni Y, Marchal G, Bogaert J, Bosmans H, Petre C, Flameng W. Localization and determination of infarct size by Gd-mesoporphyrin enhanced MRI in dogs. Int. J. Cardiac Imaging 1997; 13: 499-507; Ni Y, Pislaru C, Bosmans H, Pislaru S, Miao Y, Van de Werf F, Semmler W, Baert AL, Marchal G: Validation of intracoronary delivery of metalloporphyrin as an in vivo "histochemical staining" for myocardial infarction with MR imaging. Acad Radiolne 1998; 5(Suppl 1): S37-41; Stillman AE, Wilke N, Jerosch-Herold M. Myocardial viability. Radiologic Clinics of North America 1999; 37(2): 361; Pislaru S, Ni Y, Pislaru C, Bosmans H, Miao Y, Bogaert J, Semmler W,

Marchal G, Van de werf F. Noninvasive measurements of infarct size after thrombolysis with a necrosis-avid MRI contrast agent. Circulation 1999, 99(5): 690-696; Saeed M, Bremerich J, Wendland MF, et al. Reperfused myocardial infarction as seen with use of necrosis-specific versus standard extracellular MR contrast media in rats. Radiology 1999; 213: 247-257; Lim TH, Choi SII. MRI of myocardial infarction. JMRI 1999; 10:686-93; Wendland MF, Saeed M, Lund G, Higgins CB. Contrast-enhanced MRI for quantification of myocardial viability. JMRI 1999; 10:694-702; Choi SI, Choi SH, Kim ST, Lim KH, Lim CH, Gong GY, Kim HY, Weinmann HJ, Lim-TH. Irreversibly damaged myocardium at MR imaging with a necrotic tissue-specific contrast agent in a cat model. Radiology. 2000 Jun; 215(3): 863-8; Lee SS, Goo HW, Park SB, Lim CH, Gong G, Seo JB, and Lim TH. MR imaging of reperfused myocardial infarction: comparison of necrosis-specific and intravascular contrast agents in a cat model. Radiology 2003; 226: 739-47; Ni Y, Miao Y, Bosmans H, Yu J, Semmler W, Baert AL, Marchal G: Evaluation of interventional liver tumor ablation with Gd-mesoporphyrin enhanced magnetic resonance imaging. Radiology 1997; 205 (P):319], none of the present necrosis-avid contrast agents (NACAs) from the art have so far been commercially developed. Precedence of radio- over magneto-pharmaceutical NACAs can be a logical choice due to the negligible safety concern.

Illustrative embodiment of the invention

Legends to the graphics

Figure 1. Chemical structure of hypericin (R = H) and mono-[^{123}I]iodohypericin or MIH (R = ^{123}I).

Figure 2. SPECT transverse section images obtained in normal rats (left) and rats with reperfused hepatic infarction (right) at 24h and 48h post injection of MIH. The persistent hyperactivity is only found in the infarcted right liver

lobe from the model rat and not in the intact liver lobe of the model rat and in the liver of sham operated rat.

Figure 3. TTC staining of the liver lobe with focal reperfused infarction. From the 5 mm tissue block adjacent to the slice for autoradiography and histology (Fig. 4), the normal liver tissue (red) and necrotic tissue (pale) were sampled for radioactivity counting.

Figure 4. Comparison of autoradigraphy (left) and hematoxylin-eosin staining without (middle) and with (right) enhanced contrast and brightness of the same 50 µm frozen liver slice containing reperfused infarct from the rat.

Figure 5. SPECT images (coronal section) obtained at 24h (left) and 48h (right) post injection of MIH in a rabbit with myocardial infarction. The radioactivity can be persistently found in the heart region and to a less extent in the thyroid and gut.

Figure 6. Ex vivo images of rabbit heart. After TTC staining of a 5 mm thick slice (a), a 50-µm frozen slice (b) and corresponding autoradiographic image (c) were obtained and matched perfectly when overlapped (d). On TTC stained specimen with right ventricular wall attached (a), this transmural infarction involves the entire anterior and lateral wall of the left ventricle including the posterior papillary muscle (negative staining with TTC). On frozen slice with right ventricular wall removed (b), non-infarcted myocardium at the posterior wall and interventricular septum is stained only superficially with TTC (by the nature of this macroscopic staining technique). On autoradiography (c and d), a "doughnut" pattern of radioactive uptake appears only in the infarcted region. However, the highest activity (in red) is found mainly subendocardially and near the lateral border zone where the tracer can find its way to diffuse from the blood circulation into this occlusive myocardial infarct.

Materials en Methods

Synthesis and preparation of mono-[^{123}I]-iodohypericin (MIH)

MIH (Fig. 1) was synthesized using a standard electrophilic (radio-) iodination method in the presence of peracetic acid and was purified with high pressure liquid chromatography. Hypericin was efficiently mono-iodinated by reaction with [^{123}]iodide in the presence of peracetic acid according to Baldwin et al (Baldwin R.M. et al Nucl. Med. Biol.; 20: 597 – 606 (1993). mono-[^{123}I]-Iodohypericin is for instance obtainable by adding 150 µl of a hypericin solution in ethanol (0.5 mg/Ml) to a labeling vial containing [^{123}]NaI at pH 12, followed by 25µl 0.5M H_3PO_4, 50 µl 0.02 M peracetic acid and 50 µl ethanol. After incubation for 30 min. At room temperature, the reaction can be stopped by addition of 50 µl $NaHSO_3$ (5m/ml) and 100 µl $NaHCO_3$-solution. The ^{123}I-hypericin can be isolated and seperated from Iodide, cold hypericin and diiodohypericin by RP-HPLC on an Alltech Altima C18 3µ column eluted with a mixture of 70% ethanol and 30% 0.05M NH_4OAc at a flow rate of 1 ml/min. After chromatographic purification, the MIH solution was concentrated with a flow of nitrogen and the tracer agent was redissolved in water/polyethylene glycol (PEG) 400 (80:20, V/V) immediately before injection.

Animal models of Necrosis

All experiments were conducted with the approval of the institutional ethical committee.

1. Reperfused hepatic infarction: Three adult Wistar rats weighing 400-450 grams were anesthetized with intraperitoneal injection of pentobarbital (Nembutal®, Sanofi Sante Animale, Brussel, Belgium) at a dose of 40 mg/kg. Under laparotomy, reperfused hepatic infarction was induced by temporarily clamping the hilum of the right liver lobes for 3 hours. After reperfusion by declamping hepatic inflow, the abdominal cavity was closed with 2-layer sutures and the rats were let recovery for 8-24 h after the surgery. This relatively easy model has been successfully applied in the screening of magnetopharmaceutical NACAs before advancing to the study with myocardial infarction [Ni Y,

Petré C, Miao Y, Yu J, Cresens E, Adriaens P, Bosmans H, Semmler W, Marchal G: Magnetic resonance imaging-histomorphologic correlation studies on paramagnetic metalloporphyrins in rat models of necrosis. Invest Radiol 1997; 32(12): 770-779; Ni Y, Miao Y, Cresens E, Adriaens P, Yu J, Semmler W, Marchal G. Paramagnetic metalloporphyrins: there exist necrosis-avid and non-avid species. 7th Annual Scientific Meeting for ISMRM, Philadelphia, Pennsylvania, USA, May 22-28, 1999. Proceedings of the ISMRM Paper# 346; Ni Y, Adzamli K, Miao Y, Cresens E, Yu J, Periasamy M-P, Adams M-D, Marchal G. MRI Contrast enhancement of necrosis by MP-2269 and Gadophrin-2 in a rat model of liver infarction. Invest Radiol 2001; 36: 97-103; Ni Y, Cresens E, Adriaens P, Miao Y, Verbeke K, Dymarkoski S, Verbruggen A, Marchal G. Necrosis avid contrast agents: introducing nonporphyrin species. Acad Radiol 2002; 9 (Suppl): S98-101]. One rat received sham operation and served as non-infarcted control.

2. Occlusive myocardial infarction: A New-Zealand adult rabbit weighing about 5 kg was sedated with intramuscular injection of a mixed solution of Ketalar (ketamine hydrochloride, Parke-Davis Warner-Lambert, Belgium) at 15 mg/kg and Rompun (xylazine hydrochloride, Bayer, Levekusen, Germany) at 2.5 mg/kg. The animal was then anaesthetized with an intravenous bolus injection of Nembutal at 15 mg/kg followed by IV infusion of Nembutal at 0.1 mg/kg/min through an ear vein. Under a cold-light laryngoscope with No. 1 paediatric blade (Riester®, Jungingen, Germany), the animal was intubated with a 3.5-mm endotracheal tube, which was then connected to an artificial ventilator (Mark 7 respirator, Bird Corporation, Palm Springs, CA). An open chest surgery of left posterolateral thoracotomy was performed. The pericardium was opened to expose the left circumflex coronary artery (LCX). A loose snare loop of a 3-0 silk suture was applied around the artery and tightened with ligature. The chest was closed after evacuation of the pneumothorax.

Tracer administration

Five and 2 hours after reperfusion of the hepatic and myocardial infarction, the rat and rabbit were intravenously injected respectively with 18.5 MBq and 130 MBq of MIH through a tail vein (rat) or ear vein (rabbit).

SPECT imaging:

All imaging measurements were performed using a two-detector gamma camera (E-cam, Siemens Medical Systems, Erlangen, Germany). Each animal was secured to the head-holder of the patient bed with the organ of interest in the center of the field of view. SPECT projections were collected using the following acquisition parameters: 120 projections over 360° per detector head (step & shoot mode), 25 s per projection, a matrix size of 256x256, a pixel size of 2.4 mm, and a non-circular orbit. The images of the rats where reconstructed with filtered backprojection, using a ramp filter and cut-off at the Nyquist frequency. The images of the rabbit where reconstructed with maximum-likelihood expectation-maximization, applying 47 iterations.

In vivo SPECT was conducted under the same anesthetic regimes as that for surgeries for both the rat and rabbit. The rats were imaged consecutively during the first 2-3 hours, and then 24 and 48 hours after injection of MIH. One rat with liver lobe infarction and one sham operated control rat were placed parallel supine and imaged simultaneously. The rabbit was imaged in the similar fashion but only 24 and 48 hours after injection of MIH.

Animal Sacrifice and Tissue Sampling

Forty-eight to 60 hours post-injection, the animals were sacrificed with intravenous overdose of Nembutal. The rat liver and rabbit heart were excised. The partially necrotic part of the liver was cut into blocks of a thickness about 1 cm, which were quickly frozen in isopentane cooled over dry ice to -40°C. The heart was cut perpendicularly to the long axis into 5-mm-thick slices starting from the apex.

Histochemical Staining

Blocks of liver tissue and the slices of heart section were immersed in a buffered triphenyltetrazolium chloride (TTC) solution for staining over 10 min

at 37°C. By this staining, normal liver and myocardium tissues appeared brick red and the necrotic areas were unstained [Marchal G, Ni Y. Use of porphyrin-complex or expanded porphyrin-complex as an infarction localization diagnosticum. U.S. patent No. 6,013,241; Marchal G, Ni Y, Herijgers P, Flameng W, Petré C, Bosmans H, Yu J, Ebert W, Hilger C-S, Pfefferer D, Semmler W, Baert AL: Paramagnetic metalloporphyrins: infarct avid contrast agents for diagnosis of acute myocardial infarction by magnetic resonance imaging. Eur Radiol 1996; 6: 2-8; Ni Y, Marchal G, Herijgers P, Flameng W, Petré C, Hilger CS, Ebert W, Maier FK, Semmler W, Baert AL: Paramagnetic metalloporphyrins: from enhancers for malignant tumors to markers of myocardial infarcts. Acad Radiol 1996; 3(8): S395-397; Herijgers P, Laycock SK, Ni Y, Marchal G, Bogaert J, Bosmans H, Petre C, Flameng W. Localization and determination of infarct size by Gd-mesoporphyrin enhanced MRI in dogs. Int. J. Cardiac Imaging 1997; 13: 499-507; Ni Y, Pislaru C, Bosmans H, Pislaru S, Miao Y, Van de Werf F, Semmler W, Baert AL, Marchal G: Validation of intracoronary delivery of metalloporphyrin as an in vivo "histochemical staining" for myocardial infarction with MR imaging. Acad Radiolne 1998; 5(Suppl 1): S37-41; Stillman AE, Wilke N, Jerosch-Herold M. Myocardial viability. Radiologic Clinics of North America 1999; 37(2): 361; Pislaru S, Ni Y, Pislaru C, Bosmans H, Miao Y, Bogaert J, Semmler W, Marchal G, Van de werf F. Noninvasive measurements of infarct size after thrombolysis with a necrosis-avid MRI contrast agent. Circulation 1999, 99(5): 690-696; Saeed M, Bremerich J, Wendland MF, et al. Reperfused myocardial infarction as seen with use of necrosis-specific versus standard extracellular MR contrast media in rats. Radiology 1999; 213: 247-257; Lim TH, Choi SII. MRI of myocardial infarction. JMRI 1999; 10:686-93; Wendland MF, Saeed M, Lund G, Higgins CB. Contrast-enhanced MRI for quantification of myocardial viability. JMRI 1999; 10:694-702; Choi SI, Choi SH, Kim ST, Lim KH, Lim CH, Gong GY, Kim HY, Weinmann HJ, Lim-TH. Irreversibly damaged myocardium at MR imaging with a necrotic tissue-specific contrast agent in a cat model. Radiology. 2000 Jun; 215(3): 863-8; Lee SS, Goo HW, Park SB, Lim CH, Gong G, Seo JB, and Lim TH. MR imaging of reperfused myocardial infarction: comparison of necrosis-specific and intravascular contrast agents

in a cat model. Radiology 2003; 226: 739-47]. The TTC stained specimens were digitally photographed and stored for later imaging-histochemical match.

Ex vivo autoradiography

The frozen liver and heart tissues were cut at -20°C into 20-50 µm serial sections and exposed overnight to a high performance storage phosphor screen (Super resolution screen, Canberra-Packard, Ontario, Canada). The screen was read using a Phosphor Imager scanner (Cyclone™, Canberra-Packard). The images were analyzed using Optiquant™ software (Packard). Afterwards, these same sections were stained with haematoxylin-eosin (H&E) using the conventional procedure. These H&E stained sections were digitally scanned and the obtained images were corrected for brightness and contrast.

Tissue Radioactivity Counting

Guided by TTC staining, the liver lobes of the rat and heart sections of the rabbit were sampled for normal and necrotic parts, weighed separately and counted for radioactivity using a 3-in. NaI(Tl) scintillation detector mounted in a sample changer (Wallac Wizard, Turku, Finland). Corrections were made for background radiation and physical decay during counting. The activity in the normal and infarcted parts of the liver and heart was then expressed as activity per gram tissue.

Results

Liver lobe infarction in rats

SPECT imaging. During the first couple of hours after iv administration of MIH in both infarcted and normal control rats, a systemic distribution pattern appeared with higher activity uptake seen especially in the liver and kidneys, indicating the major elimination pathways of the compound. In comparison with a complete outline of the liver in the normal rat, there was a filling defect at the lower right quadrant of the liver, corresponding to the induced liver infarction. At 24 h as well as 48 h post injection, on the transversal SPECT image, the uptake of radioactivity in the infarcted liver lobe was apparently much higher than that in the noninfarcted liver lobe and in the liver of the sham operated rat (Fig. 2). Residual radioactivity was also shown in the regions of thyroid and intestines.

Tissue radioactivity counting. Sixty hours post injection of the compound, the results of radioactivity quantification showed a specific uptake in the necrotic liver lobe of 3.51 %ID/g, which was almost 10 times the amount found in the untreated lobes (0.38 %ID/g). Furthermore, the amount in the liver lobes of the control rat was comparable to the amount found in the untreated liver lobes of the rat with infarction (0.58 %ID/g).

Histochemical Staining. Figure 3 shows a picture of 0.5 cm thick block of the partially necrotic liver of the rat. After staining with TTC, the reddish normal liver and adjacent pale necrotic tissue could be easily identified, which was confirmed by H&E staining of the 50-µm serial sections taken from 5 mm next to this slice (Fig. 4).

Ex vivo autoradiography: On autoradiographic scales, areas with high activity appear red, while areas with low activity appear gray to white. Fig. 4 compares the outcomes of autoradiography and H&E staining from the same 50-µm sections. The hyperactivity appears only in the pink colored (eosinophilic) necrotic parts, whereas the hypoactivity is found in the purple colored (hematoxylinophilic) healthy parts of the liver. The topographic distribution of the radioactivity matches perfectly with that of the necrotic

tissue components, suggesting that MIH specifically accumulates in necrotic tissue (Fig. 4).

Myocardial infarction in the rabbit

In Vivo SPECT imaging: Twenty four to 48 hours post injection of MIH in the rabbit with occlusive myocardial infarction, coronal section view after iterative reconstruction of whole body SPECT persistently displayed only one hot spot in the anatomical area of the heart. Radioactivity to a much lesser extent could also be clearly shown in the regions of thyroid and intestines (Fig. 5).

Tissue radioactivity counting: TTC staining enabled selective sampling of reddish normal myocardium and whitish infarcted myocardium for radioactivity quantification. The results showed a 18-fold higher accumulation in the infarcted tissue (X %ID/g) than in the healthy tissue (Y %ID/g). The ratio could be even much higher, if tissue sampling had been guided by the outcome of autoradiography in this model of occlusive myocardial infarction (Fig. 6).

Ex vivo histochemical staining and autoradiography: Figure 6 compares TTC staining of a 5 mm thick slice, a 50-µm frozen slice with corresponding autoradiographic image and their superimposed effect. On TTC stained specimen with right ventricular wall attached (Fig.6a), the transmural infarction involves the entire anterior and lateral wall of the left ventricle including the posterior papillary muscle (negative staining with TTC). On frozen slice with right ventricular wall removed (Fig.6b), normal myocardium at the posterior wall and interventricular septum is stained only superficially with TTC (by the nature of this macroscopic staining technique). On autoradiography (Fig.6c,d), a "doughnut" pattern of radioactive uptake appears only in the infarcted region. However, the highest activity (in red) is found mainly subendocardially and near the lateral border zone, a sign characteristic for occlusive myocardial infarct [Ni Y, Dymarkowski S, Chen F, Bogaert J, and Marchal G. Occlusive myocardial infarction: enhanced or not enhanced with necrosis avid contrast agents at magnetic resonance imaging. Radiology 2002; 225: 603-5].

Discussion

Experiments on mammalian models by meticulous and accurate methodologies applied clearly demonstrated for the first time and proved that MIH proves to be a highly sensitive/ specific necrosis-avid and clinical applicable agent.

As hypericin is a polyphenolic anthraquinone derivative, it can be labelled efficiently and quite simply with radioiodine by electrophilic substitution in ortho position of a phenol [G. Lavie, Y. Mazur, D. Lavie and D. Meruelo , The chemical and biological properties of hypericin: a compound with a broad spectrum of biological activities. Med. Res. Rev. 15 (1995), pp. 111–119; Vanbilloen H, Bormans G, Chen B, de Witte P, Verbruggen A, Verbeke K. Synthesis and preliminary evaluation of mono-[^{123}I]iodohypericin. *J* Labelled Comp Radiopharm. 2001;44: S965-S967]. Structural analysis of the radioiodinated derivative has shown that in this way one iodine-123 radionuclide is reproducibly introduced on carbon atom 2, in ortho position of the phenolic group with the most acidic characteristics (Fig. 1). The so formed mono-[^{123}I]iodohypericin (MIH) could efficiently be separated from the starting material hypericin by reversed phase HPLC and was obtained with an over 99% purity in non-carrier added form. After intravenous injection in rats, gamma camera images showed that MIH was rapidly distributed over the whole body, with early visualization of blood pool, liver and kidneys, followed by intestines and to a lesser degree urinary bladder. At 24 h and 48 h after injection, there is a clear accumulation of MIH in a well-defined area of the liver of the rats with induced infarction; whereas in the untreated rat, an even distribution over the liver region is seen at these time points (Fig. 2). As hypericin and MIH are very lipophilic compounds, their excretion through liver and intestines is quite high [Vanbilloen H, Bormans G, Chen B, de Witte P, Verbruggen A, Verbeke K. Synthesis and preliminary evaluation of mono-[^{123}I]iodohypericin. *J* Labelled Comp Radiopharm. 2001;44: S965-S967] and for this reason, the clear visualization of a hot spot in the liver is even more remarkable, indicating a high target to non-target ratio. Confirmation that this preferential activity uptake was in the infarcted tissue was obtained by comparison of the images generated with TTC staining, H&E staining and

autoradiography of blocks from excised liver lobes after sacrifice of the animal over 48 h post injection. There is a perfect correlation between the distribution of radioactivity seen on the autoradiographic image of infarcted liver tissue and the areas stained with haematoxylin-eosin, the latter verifying the presence of necrotic tissue (Fig. 4). The same holds true for the images obtained after staining with TTC (Fig. 3). Comparison of the activity per gram tissue in infarcted liver tissue over that in normal liver tissue reveals a 10-times higher radioactivity concentration in the infarcted area. This is a clear indication that the new tracer agent MIH has indeed a high affinity for necrotic tissue.

The suitability of MIH for visualisation of necrotic myocardial tissue was confirmed using a rabbit model of myocardial infarction. Also in the rabbit study a remarkable hot spot was visible in the region of the myocardial infarction, both at 24 h and 48 h post injection (Fig. 5,6). As in the rat study a perfect correlation was found between the areas stained by TTC and the areas with higher uptake of radioactivity. The target (necrotic myocardium) to non-target (normal myocardium) ratio was even significantly higher than in the case of the rat liver, namely a factor of 18. This ratio could be even well increased if more accurate tissue sampling had been performed at the subendocardial region that entails higher activity in this model of occlusive myocardial infarction (Fig. 6).

Despite a lack of sufficient spatial resolution of the in vivo SPECT images in the rat and rabbit due to clinical calibrations of the equipment, ex vivo autoradiography in combination with histochemical staining techniques convincingly confirmed the specific accumulation of MIH in infarcted liver and myocardium. Indeed, being able to display detailed uptake patterns such as the present "doughnut sign" implies a capability of differential diagnosis between occlusive and reperfused myocardial infarction with MIH mediated imaging modalities, which is crucial for making a clinical decision of prompt interventions for coronary revascularization [Ni Y, Dymarkowski S, Chen F, Bogaert J, and Marchal G. Occlusive myocardial infarction: enhanced or not enhanced with necrosis avid contrast agents at magnetic resonance imaging. Radiology 2002; 225: 603-5; Rude R, Parkey RW, Bonte FJ, et al. Clinical

implication of the "doughnut" pattern of uptake in myocardial imaging with technetium-99 stannous pyrophosphate. Circulation 1977; 56:m-561].

Non-invasive "hot spot imaging" and localization of necrotic tissue may be helpful for the diagnosis of different disorders. This is especially true in the case of ischemic myocardial injury, where imaging using necrosis avid agents could help in measuring infarct size. This can allow the rapid use of interventions for myocardial salvage through early identification of the acute event, in this way improving the clinical outcome. Also other cardiovascular disorders associated with cardiac cell death can be visualized and diagnosed, such as cardiomyopathies, myocarditis and heart transplant rejection [Flotats A, Carrió I. Non-invasive in vivo imaging of myocardial apotosis and necrosis. Eur J Nucl Med Mol Imaging. 2003;30:615-630.].

In Nuclear Medicine, only a limited number of "hot spot imaging" agents for targeting necrosis have been used or proposed. ^{99m}Tc-pyrophosphate was the first of them and is supposed to bind to necrotic myocardial tissue by targeting calcium phosphate deposited in the mitochondria of infarcted or severely injured myocardial tissue [Rude R, Parkey RW, Bonte FJ, et al. Clinical implication of the "doughnut" pattern of uptake in myocardial imaging with technetium-99 stannous pyrophosphate. Circulation 1977; 56:m-561; Buja LM, Tofe AJ, Kulkarni PV et al. Sites and mechanisms of localization of technetium-99m phosphorous radiopharmaceuticals in acute myocardial infarcts and other tissues. J Clin Invest. 1977; 60:724-740.]. However, ^{99m}Tc-pyrophosphate scintigraphy has never gained widespread use because of its limited diagnostic accuracy and relatively poor stability that may lead to the presence of pertechnetate and so result in imaging of the cardiac chambers. More recently, ^{111}In-labeled murine monoclonal antimyosin Fab antibody fragments were introduced for infarct-avid scintigraphy [Khaw BA, Gold HK, Fallon JT, et al. Scintigraphic quantification of myocardial necrosis in patients after intravenous injectiuon of cardiac myosin specific antibody. Circulation. 1986; 74:501-508; Khaw BA, Yasuda T, Gold HK, et al. Acute myocardial infarction imaging with indium-111 labeled monoclonal antimyosin Fab fragments. J Nucl Med. 1987; 28:1671-1678]. This so-called ^{111}In-antimyosin has a selective affinity for the intracellular heavy chain of cardiac myosin, which is exposed when the integrity of the sarcolemma is lost as a result of

cell damage [Khaw BA, Fallon JT, Beller GA, Haber E. Specificity of localization of myosin-specific antibody fragments in experimental myocardial infarction: histologic, histochemical, autoradiographic and scintigraphic studies. Circulation 1979 ;60 :1527-1531; Khaw BA, Scott J, Fallon JT, et al. Myocardial injury: quantitation by cell sorting initiated with antimyosin fluorescent spheres. Science. 1982;217:1050-1053]. It is incorporated in the necrotic myocardium in an inverse relationship to regional flow, with maximum uptake in areas with severe flow impairment, although its uptake is more intense in myocardial infarcts with reperfusion than in those with persistent coronary occlusion [Frist W, Yasuda T, Segall G, et al. Noninvasive detection of human cardiac transplant rejection with indium-111 anti-myosin (Fab) imaging. Circulation 1987; 76 (Suppl V): 81-5]. It was also found useful for detection of acute or chronic diffuse myocardial damage in allograft rejection in cardiac transplantation [Frist W, Yasuda T, Segall G, et al. Noninvasive detection of human cardiac transplant rejection with indium-111 anti-myosin (Fab) imaging. Circulation 1987; 76 (Suppl V): 81-5.], doxorubicin-induced cardiotoxicity [Ballester M, Obrador D, Carrio I, et al. ^{111}In-monoclonal antimyosin antibody studies after the first year of heart transplantation: identification of risk groups for developing rejection during long-term follow-up and clinical implications. Circulation. 1990;82:2100-2108; Ballester M, Bordes R, Tazelaar T, et al. Evaluation of biopsy classification for rejection: relation to the detection of myocardial damage by ^{111}In-monoclonal antimyosin antibody imaging. J Am Coll Cardiol. 1998;31:1357-1361], acute myocarditis [Dec GW, Palacios IF, Yasuda T, et al. Antimyosin antibody cardiac imaging: its role in the diagnosis of myocarditis. J Am Coll Cardiol. 1990;6:97-104; Narula J, Khaw BA, Dec GW, et al. Recognition of acute myocarditis masquerading as acute myocardial infarction. N Engl J Med. 1992;328:100-104] and various cardiomyopathies [Obrador D, Ballester M, Carrio I, et al. Active myocardial damage without attending inflammatory response in idiopathic dilated cardiomyopathy. J Am Coll Cardiol. 1993;21:1667-1671; Obrador D, Ballester M, Carrio I, et al. Presence, evolving changes, and prognostic implications of myocardial damage detected in idiopathic and alcoholic dilated cardiomyopathy by^{111}In monoclonal antimyosin antibodies. Circulation. 1994;89:2054-2061]. Although ^{111}In-antimyosin was recently approved by the

FDA for clinical use, the limitation of approved indications to ischemic heart disease has resulted in cessation of commercial production.

Very recently, it was observed that the complex of ^{99m}Tc with glucaric acid, a simple dicarboxylic acid sugar, localized in canine reperfused myocardial infarction soon after injection [Narula J, Petrov A, Pak KY, et al. Very early noninvasive detection of acute experimental nonreperfused myocardial infarction with ^{99m}Tc-labeled glucarate. Circulation. 1995;95:1577-1584]. The tracer agent is supposed to bind to positively charged histones within disintegrated nuclei and reduced subcellular organelle proteins in necrotic myocytes [Khaw BA, Nakazama A, O'Donell SM, et al. Avidity of technetium-99m glucarate for the necrotic myocardium: in vivo and in vitro assessment. J Nucl Cardiol. 1997;4:283.290]. It has the advantage of a rapid blood pool clearance, a good target to background ratio, lack of toxicity and antigenicity and is claimed to have a good sensitivity and specificity for detection of early irreversible myocyte injury. On the other hand, its uptake is limited to the first 9 hours after the onset of acute myocardial infarction because of the relatively rapid disintegration of the positively charged histones. Further clinical trials have to reveal its real clinical usefulness.

Although potential clinical impact of such a necrosis-targeting approach has been repeatedly emphasized in the literature [Ni Y, Marchal G, Yu J, Lukito G, Petré C, Wevers M, Baert AL, Ebert W, Hilger CS, Maier FK, Semmler W: Localization of metalloporphyrin induced "specific" enhancement in experimental liver tumors: a comparison between MRI, microangiographic and histologic findings. Acad Radiol 1995; 2: 687-699; Ni Y, Petré C, Miao Y, Yu J, Cresens E, Adriaens P, Bosmans H, Semmler W, Marchal G: Magnetic resonance imaging-histomorphologic correlation studies on paramagnetic metalloporphyrins in rat models of necrosis. Invest Radiol 1997; 32(12): 770-779; Maurer J, Strauss A, Ebert W, Bauer H, Felix R. Contrast-enhanced high resolution magnetic resonance imaging of pigmented malignant melanoma using Mn-TPPS4 and Gd-DTPA: experimental results. Melanoma Res 2000; 10: 40-6; Marchal G, Ni Y. Use of porphyrin-complex or expanded porphyrin-complex as an infarction localization diagnosticum. U.S. patent No. 6,013,241; Marchal G, Ni Y, Herijgers P, Flameng W, Petré C, Bosmans H, Yu J, Ebert W, Hilger C-S, Pfefferer D, Semmler W, Baert AL: Paramagnetic

metalloporphyrins: infarct avid contrast agents for diagnosis of acute myocardial infarction by magnetic resonance imaging. Eur Radiol 1996; 6: 2-8; Ni Y, Marchal G, Herijgers P, Flameng W, Petré C, Hilger CS, Ebert W, Maier FK, Semmler W, Baert AL: Paramagnetic metalloporphyrins: from enhancers for malignant tumors to markers of myocardial infarcts. Acad Radiol 1996; 3(8): S395-397; Herijgers P, Laycock SK, Ni Y, Marchal G, Bogaert J, Bosmans H, Petre C, Flameng W. Localization and determination of infarct size by Gd-mesoporphyrin enhanced MRI in dogs. Int. J. Cardiac Imaging 1997; 13: 499-507; Ni Y, Pislaru C, Bosmans H, Pislaru S, Miao Y, Van de Werf F, Semmler W, Baert AL, Marchal G: Validation of intracoronary delivery of metalloporphyrin as an in vivo "histochemical staining" for myocardial infarction with MR imaging. Acad Radiolne 1998; 5(Suppl 1): S37-41; Stillman AE, Wilke N, Jerosch-Herold M. Myocardial viability. Radiologic Clinics of North America 1999; 37(2): 361; Pislaru S, Ni Y, Pislaru C, Bosmans H, Miao Y, Bogaert J, Semmler W, Marchal G, Van de werf F. Noninvasive measurements of infarct size after thrombolysis with a necrosis-avid MRI contrast agent. Circulation 1999, 99(5): 690-696; Saeed M, Bremerich J, Wendland MF, et al. Reperfused myocardial infarction as seen with use of necrosis-specific versus standard extracellular MR contrast media in rats. Radiology 1999; 213: 247-257; Lim TH, Choi SII. MRI of myocardial infarction. JMRI 1999; 10:686-93; Wendland MF, Saeed M, Lund G, Higgins CB. Contrast-enhanced MRI for quantification of myocardial viability. JMRI 1999; 10:694-702; Choi SI, Choi SH, Kim ST, Lim KH, Lim CH, Gong GY, Kim HY, Weinmann HJ, Lim-TH. Irreversibly damaged myocardium at MR imaging with a necrotic tissue-specific contrast agent in a cat model. Radiology. 2000 Jun; 215(3): 863-8; Lee SS, Goo HW, Park SB, Lim CH, Gong G, Seo JB, and Lim TH. MR imaging of reperfused myocardial infarction: comparison of necrosis-specific and intravascular contrast agents in a cat model. Radiology 2003; 226: 739-47; Ni Y, Miao Y, Bosmans H, Yu J, Semmler W, Baert AL, Marchal G: Evaluation of interventional liver tumor ablation with Gd-mesoporphyrin enhanced magnetic resonance imaging. Radiology 1997; 205 (P):319], none of the NACAs for MRI have so far been commercialized. Precedence of radio- over magneto-pharmaceutical NACAs can be a logical choice due to the negligible safety concern. In comparison to other existing

necrosis-avid tracers for nuclear imaging and NACAs for MRI, developing and using hypericin derivatives of this type can be advantageous, because 1) hypericin is one of the most popular naturally obtainable medicines already widely applied for over millennia with favourable biocompatibility and safety profile; 2) the procedure for preparing radioactive hypericin is much simpler and therefore more economical than that for antibody tracers.

Regarding the mechanisms behind the observed necrosis-avidity, there exist more hypotheses than solid experimental proofs [Ni Y, Marchal G, Yu J, Lukito G, Petré C, Wevers M, Baert AL, Ebert W, Hilger CS, Maier FK, Semmler W: Localization of metalloporphyrin induced "specific" enhancement in experimental liver tumors: a comparison between MRI, microangiographic and histologic findings. Acad Radiol 1995; 2: 687-699; Ni Y, Petré C, Miao Y, Yu J, Cresens E, Adriaens P, Bosmans H, Semmler W, Marchal G: Magnetic resonance imaging-histomorphologic correlation studies on paramagnetic metalloporphyrins in rat models of necrosis. Invest Radiol 1997; 32(12): 770-779; Maurer J, Strauss A, Ebert W, Bauer H, Felix R. Contrast-enhanced high resolution magnetic resonance imaging of pigmented malignant melanoma using Mn-TPPS4 and Gd-DTPA: experimental results. Melanoma Res 2000; 10: 40-6; Marchal G, Ni Y. Use of porphyrin-complex or expanded porphyrin-complex as an infarction localization diagnosticum. U.S. patent No. 6,013,241; Marchal G, Ni Y, Herijgers P, Flameng W, Petré C, Bosmans H, Yu J, Ebert W, Hilger C-S, Pfefferer D, Semmler W, Baert AL: Paramagnetic metalloporphyrins: infarct avid contrast agents for diagnosis of acute myocardial infarction by magnetic resonance imaging. Eur Radiol 1996; 6: 2-8; Ni Y, Marchal G, Herijgers P, Flameng W, Petré C, Hilger CS, Ebert W, Maier FK, Semmler W, Baert AL: Paramagnetic metalloporphyrins: from enhancers for malignant tumors to markers of myocardial infarcts. Acad Radiol 1996; 3(8): S395-397; Herijgers P, Laycock SK, Ni Y, Marchal G, Bogaert J, Bosmans H, Petre C, Flameng W. Localization and determination of infarct size by Gd-mesoporphyrin enhanced MRI in dogs. Int. J. Cardiac Imaging 1997; 13: 499-507; Ni Y, Pislaru C, Bosmans H, Pislaru S, Miao Y, Van de Werf F, Semmler W, Baert AL, Marchal G: Validation of intracoronary delivery of metalloporphyrin as an in vivo "histochemical staining" for myocardial infarction with MR imaging. Acad Radiolne 1998; 5(Suppl 1): S37-

41; Stillman AE, Wilke N, Jerosch-Herold M. Myocardial viability. Radiologic Clinics of North America 1999; 37(2): 361; Pislaru S, Ni Y, Pislaru C, Bosmans H, Miao Y, Bogaert J, Semmler W, Marchal G, Van de werf F. Noninvasive measurements of infarct size after thrombolysis with a necrosis-avid MRI contrast agent. Circulation 1999, 99(5): 690-696; Saeed M, Bremerich J, Wendland MF, et al. Reperfused myocardial infarction as seen with use of necrosis-specific versus standard extracellular MR contrast media in rats. Radiology 1999; 213: 247-257; Lim TH, Choi SII. MRI of myocardial infarction. JMRI 1999; 10:686-93; Wendland MF, Saeed M, Lund G, Higgins CB. Contrast-enhanced MRI for quantification of myocardial viability. JMRI 1999; 10:694-702; Choi SI; Choi SH, Kim ST, Lim KH, Lim CH, Gong GY, Kim HY, Weinmann HJ, Lim-TH. Irreversibly damaged myocardium at MR imaging with a necrotic tissue-specific contrast agent in a cat model. Radiology. 2000 Jun; 215(3): 863-8; Lee SS, Goo HW, Park SB, Lim CH, Gong G, Seo JB, and Lim TH. MR imaging of reperfused myocardial infarction: comparison of necrosis-specific and intravascular contrast agents in a cat model. Radiology 2003; 226: 739-47; Ni Y, Miao Y, Bosmans H, Yu J, Semmler W, Baert AL, Marchal G: Evaluation of interventional liver tumor ablation with Gd-mesoporphyrin enhanced magnetic resonance imaging. Radiology 1997; 205 (P):319; Ni Y, Miao Y, Cresens E, Adriaens P, Yu J, Semmler W, Marchal G, Paramagnetic metalloporphyrins: there exist necrosis-avid and non-avid species. 7th Annual Scientific Meeting for ISMRM, Philadelphia, Pennsylvania, USA, May 22-28, 1999. Proceedings of the ISMRM Paper# 346, Ni Y, Adzamli K, Miao Y, Cresens E, Yu J, Periasamy M-P, Adams M-D, Marchal G. MRI Contrast enhancement of necrosis by MP-2269 and Gadophrin-2 in a rat model of liver infarction. Invest Radiol 2001; 36: 97-103; Ni Y, Cresens E, Adriaens P, Miao Y, Verbeke K, Dymarkoski S, Verbruggen A, Marchal G. Necrosis avid contrast agents: introducing nonporphyrin species. Acad Radiol 2002; 9 (Suppl): S98-101; Ni Y, Dymarkowski S, Chen F, Bogaert J, and Marchal G. Occlusive myocardial infarction: enhanced or not enhanced with necrosis avid contrast agents at magnetic resonance imaging. Radiology 2002; 225: 603-5; Rude R, Parkey RW, Bonte FJ, et al. Clinical implication of the "doughnut" pattern of uptake in myocardial imaging with technetium-99 stannous pyrophosphate. Circulation 1977; 56:m-561;

Flotats A, Carrió I. Non-invasive in vivo imaging of myocardial apotosis and necrosis. Eur J Nucl Med Mol Imaging. 2003;30:615-630; Buja LM, Tofe AJ, Kulkarni PV et al. Sites and mechanisms of localization of technetium-99m phosphorous radiopharmaceuticals in acute myocardial infarcts and other tissues. J Clin Invest. 1977; 60:724-740; Khaw BA. The current role of infarct avid imaging. Semin Nucl Med. 1999;29:259-270; Narula J, Petrov A, Pak KY, et al. Very early noninvasive detection of acute experimental nonreperfused myocardial infarction with ^{99m}Tc-labeled glucarate. Circulation. 1995;95:1577-1584; Khaw BA, Nakazama A, O'Donell SM, et al. Avidity of technetium-99m glucarate for the necrotic myocardium: in vivo and in vitro assessment. J Nucl Cardiol. 1997;4:283.290]. Despite a great diversity in chemical structures among various necrosis-avid tracer agents for nuclear medicine and NACAs for MRI, common physicochemical interactions should be shared by at lease some of these agents. However, it is unlikely that MIH and ^{99m}Tc-pyrophosphate would interact in a similar manner with necrotic components because skeletal uptake characteristic for ^{99m}Tc-pyrophosphate was not evidenced with MIH in the present study. Therefore, specificity of MIH for myocardial infarction should be higher than that of ^{99m}Tc-pyrophosphate that also reactive to many other noninfarct calcium-enriched conditions under a likely different targeting mechanism [Buja LM, Tofe AJ, Kulkarni PV et al. Sites and mechanisms of localization of technetium-99m phosphorous radiopharmaceuticals in acute myocardial infarcts and other tissues. J Clin Invest. 1977; 60:724-740].

Compounds and derivatives with a structure-function relationship with hypericine and more specifically especially a similarity in local configurations instead of global skeletons can have similar necrosis specific and infarct specific properties.

The present study suggests that in addition to the claimed anti-depressive, anti-microbial and anti-neoplastic activities, hypericin and hypericin derivatives can serve as powerful necrosis avid diagnostic agents for tissue viability assessment and as targeting carriers for tissue revival therapies.

Figures

Figure 1. Chemical structure of hypericin (R = H) and mono-[^{123}I]iodohypericin or MIH (R = ^{123}I).

Figure 2. SPECT transverse section images obtained in normal rats (left) and rats with reperfused hepatic infarction (right) at 24h and 48h post injection of MIH. The persistent hyperactivity is only found in the infarcted right liver lobe from the model rat and not in the intact liver lobe of the model rat and in the liver of sham operated rat.

Figure 3. TTC staining of the liver lobe with focal reperfused infarction. From the 5 mm tissue block adjacent to the slice for autoradiography and histology (Fig. 4), the normal liver tissue (red) and necrotic tissue (pale) were sampled for radioactivity counting.

Figure 4. Comparison of autoradigraphy (left) and hematoxylin-eosin staining without (middle) and with (right) enhanced contrast and brightness of the same 50 µm frozen liver slice containing reperfused infarct from the rat.

Figure 5. SPECT images (coronal section) obtained at 24h (left) and 48h (right) post injection of MIH in a rabbit with myocardial infarction. The radioactivity can be persistently found in the heart region and to a less extent in the thyroid and gut.

Figure 6. Ex vivo images of rabbit heart. After TTC staining of a 5 mm thick slice (a), a 50-µm frozen slice (b) and corresponding autoradiographic image (c) were obtained and matched perfectly when overlapped (d). On TTC stained specimen with right ventricular wall attached (a), this transmural infarction involves the entire anterior and lateral wall of the left ventricle including the posterior papillary muscle (negative staining with TTC). On frozen slice with right ventricular wall removed (b), non-infarcted myocardium at the posterior wall and interventricular septum is stained only superficially with TTC (by the nature of this macroscopic staining technique). On autoradiography (c and d), a "doughnut" pattern of radioactive uptake appears only in the infarcted region. However, the highest activity (in red) is found mainly subendocardially and near the lateral border zone where the tracer can

find its way to diffuse from the blood circulation into this occlusive myocardial infarct.

Tissue Infarction or Necrosis Specific compounds

Abstract

To verify the hypothesis that the naturally occurring compound hypericin, a polycyclic quinone found in St. Johns Wort (*Hypericum perforatum*), may function as a necrosis avid agent for diagnostic and therapeutic purposes, the radioactive mono-[^{123}I]-iodohypericin (MIH) was prepared and evaluated in animal models of liver infarction in the rat and heart infarction in the rabbit using single photon emission computered tomography (SPECT), serial sectional autoradiography and microscopy, TTC histochemical staining, and radioactivity counting techniques. The hepatic and cardiac infarction was persistently visualized with in vivo SPECT as well defined hot spots over 48 h, which could be proven topographically by postmortem TTC staining, autoradiography and histology, and quantitatively by a ratio of 10 times higher radioactivity counting in necrotic over normal liver tissues and 18 times in infarcted over normal myocardium. The present study suggests that in addition to the previously claimed anti-depressive, anti-microbial and anti-neoplastic activities, hypericin derivatives may serve as powerful necrosis avid diagnostic agents for tissue viability assessment and potentially as targeting vectors for tissue revival therapies.

Figure 1.

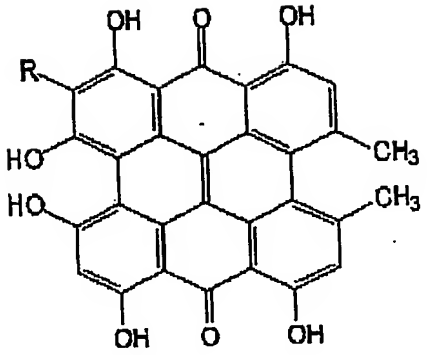

Figure 2.

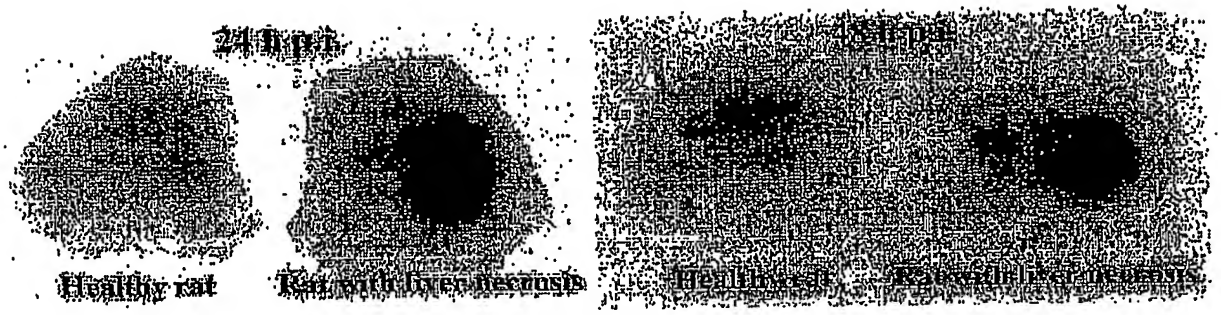

Figure 3.

Figure 4.

Figure 5.

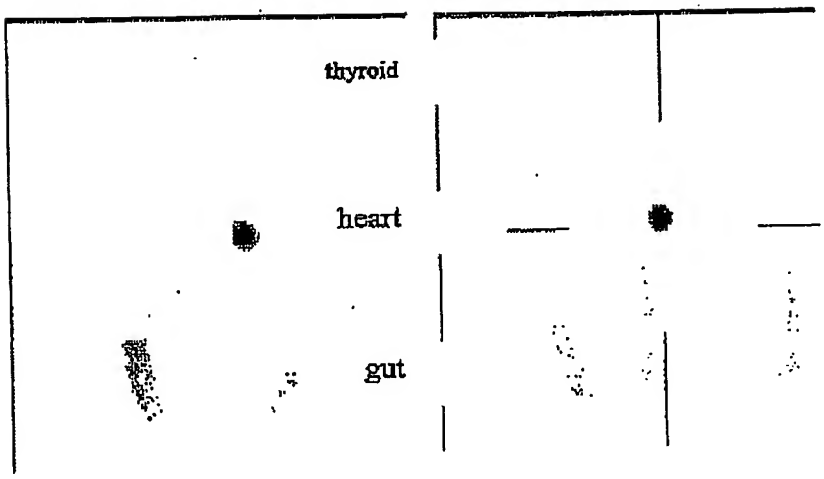

Figure 6.